Modified voltage model and high frequency signal injection

This chapter presents an algorithm to estimate the rotor position and speed for Permanent Magnet Synchronous machines. The algorithm is based on modified voltage model (at high speed), combined with high frequency signal injection at low speed (from stand still). A pure voltage model of the machine is first derived, and then modified afterwards to achieve good performance of the algorithm. Simulation results done in Simulink show that the algorithm works for Surface Mounted Permanent Magnet Motor.

6.1 Pure voltage model of the machine

A pure voltage model of the Permanent Magnet Motor can be made of set of two equations, the back-EMF equation and the rotor flux equation. Consider equations (1) and (2) presented in chapter two, (see Permanent Magnet Motor model). These equations can be used to formulate the estimated voltage and flux equations of the PM motor in the estimated dq rotor reference frame as presented bellow.

$$\begin{aligned} V_d &= \hat{R}_s i_d + \frac{d\hat{\lambda}_d}{dt} - \hat{\omega}_m \hat{\lambda}_q \\ V_q &= \hat{R}_s i_q + \frac{d\hat{\lambda}_q}{dt} + \hat{\omega}_m \hat{\lambda}_d \end{aligned} \tag{18}$$

$$\begin{aligned} \hat{\lambda}_d &= \hat{L}_d i_d + \hat{\lambda}_m \\ \hat{\lambda}_q &= \hat{L}_q i_q \end{aligned} \tag{19}$$

The estimated quantities are marked with the signe $\wedge$. After reading the previous chapter, two important aspects to keep in mind when deriving PM machine model could be emphasized:

- the rotor magnet flux is aligned with the rotor d-axis
- the back-EMF in the machine always lies on the rotor q-axis

Since the rotor permanent magnet flux is aligned with the rotor d-axis, the d-axis component of the machine voltage in equation (18) can be used to derive the estimated rotor flux of the machine.
Substituting equation (19) in equation (18) and solving for the permanent magnet flux variation will result in equation (20).

$$\frac{d\hat{\lambda}_m}{dt} = V_d - \hat{R}_s i_d - \hat{L}_d \frac{di_d}{dt} + \hat{\omega}_m \hat{L}_d i_q \tag{20}$$

In the same order, for the reason that the back-EMF in the machine always lies on the rotor q-axis, the q-axis component of the machine voltage in equation (18) can be used to derive the estimated back-EMF of the motor in the rotor dq reference frame.

$$\begin{aligned} V_q &= \hat{R}_s i_q + \hat{L}_q \frac{di_q}{dt} + \hat{\omega}_m \hat{L}_d i_d + \hat{\omega}_m \hat{\lambda}_m \\ &= \hat{R}_s i_q + \hat{L}_q \frac{di_q}{dt} + \hat{\omega}_m \hat{L}_d i_d + \hat{e}_q \end{aligned} \tag{21}$$

Where $\hat{e}_q = \hat{\omega}_m \hat{\lambda}_m$ stands for the estimated back-EMF of the machine.

Solving equation (21) for $\hat{e}_q$ will result in the following:

$$\hat{e}_q = V_q - \hat{R}_s i_q - \hat{L}_q \frac{di_q}{dt} - \hat{\omega}_m \hat{L}_d i_d \tag{22}$$

A pure voltage model of the Permanent magnet machine can be described by the set of equations (20) and (22).

Obtained pure voltage model of de machine:

$$\begin{aligned} \frac{d\hat{\lambda}_m}{dt} &= V_d - \hat{R}_s i_d - \hat{L}_d \frac{di_d}{dt} + \hat{\omega}_m \hat{L}_d i_q \\ \hat{e}_q &= V_q - \hat{R}_s i_q - \hat{L}_q \frac{di_q}{dt} - \hat{\omega}_m \hat{L}_d i_d \end{aligned} \tag{23}$$

The pure voltage model of the Permanent magnet machine suffers from output drifts due to the open loop integration [6]. Therefore, an adjustment is required in order to prevent from the integration drifts, thereby obtaining the so called modified voltage model (as mentioned in the title of this chapter).

One way to prevent from integration drifts in the voltage model of the machine is to add to the pure voltage model an offset term contained in the input of the model [6]. The offset term can be described by the following equation.

$$\hat{u}_{off} = k(\lambda_{m\_ref} - \hat{\lambda}_m) \tag{24}$$

Where k is a non negative gain, and λ_{m_ref} the reference permanent magnet flux term.
The modified machine voltage equation is obtained by adding equation (24) to the upper term of equation (23).

Obtained modified voltage model of the machine:

$$\begin{aligned} \frac{d\hat{\lambda}_m}{dt} &= V_d - \hat{R}_s i_d - \hat{L}_d \frac{di_d}{dt} + \hat{\omega}_m \hat{L}_d i_q + k(\lambda_{m\_ref} - \hat{\lambda}_m) \\ \hat{e}_q &= V_q - \hat{R}_s i_q - \hat{L}_q \frac{di_q}{dt} - \hat{\omega}_m \hat{L}_d i_d \end{aligned} \tag{25}$$

6.1.1 Estimated rotor speed and position

In equation (21), the estimated back-EMF term was described by the following equation:

$$\hat{e}_q = \hat{\omega}_m \hat{\lambda}_m \tag{26}$$

$$\text{Then,} \quad \hat{\omega}_m = \frac{\hat{e}_q}{\hat{\lambda}_m} \tag{27}$$

Equation (27) describes the estimated rotational angular velocity of the rotor.
Obviously, the estimated rotor position is obtained by integrating the estimated rotor speed.

6.2 High frequency signal injection

Alternating voltages can be used for high frequency signal injection [10-12]. The signal injection model used in this project is made of a carrier

signal fluctuating at the angular frequency $\omega_i = 2\pi f_i$ where f_i is the injected high frequency.
The injected voltage signal can be described as in the following equation:

$$u_i(t) = \hat{u}_{\max} \cos \omega_i t \tag{28}$$

Where $\hat{u}_{\max}$ and f_i are to be set to the proper values depending on the project specifications and the case of study applied to fulfill the project requirements. In this project, these quantities are obtained by experimental simulations.
The signal $u_i(t)$ is superimposed on the d-axis component of the voltage in the estimated rotor reference frame.
An alternating high frequency current response is detected in the q-direction of the estimated rotor reference frame, amplitude modulated by the rotor position estimation error [4].
The demodulation principle is shown in the figure below [4].

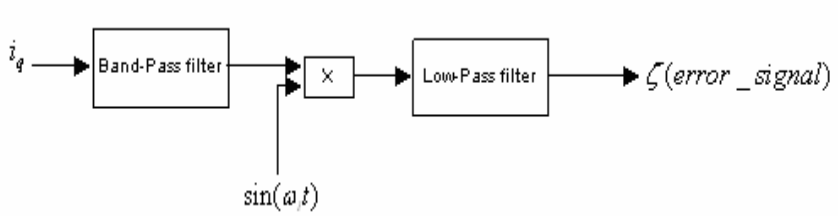

Figure 6.1: *Demodulation principle of the error signal contained in the q-axis current*

The q-axis current component of the measured current is band-pass filtered and forced to oscillate (alternatively) at the injected high frequency, then low-pass filtered to extract its fundamental component (error signal), which is function dependent of the error in the estimated rotor position. The equation describing the error signal, taken on an ideal basis is presented below [4].

$$\zeta = \frac{\hat{u}_{\max}}{\omega_i}\left[\frac{L_{q-}L_d}{4L_qL_d}\right]\sin(2\tilde{\theta}_m) \tag{29}$$

Where $\tilde{\theta}_m = \theta_m - \hat{\theta}_m$, is the estimated error of the rotor position.

It is clear from equation (29) that ideally, if there is no error in the estimated rotor position ($\tilde{\theta}_m = 0$), the error signal will be zero ($\zeta = 0$).
This aspect appears to be valid for surface mounted permanent magnet motors, considering the steady state machine inductance equality ($L_d = L_q$).
However, all types of PM machines own a little saliency (on the real basis), providing that $L_d \neq L_q$.

The filters used in figure (6.1) can be continuous time filters or discrete filters. Discrete filters are the types applied to this project since their design (which is not shown here) can easily be done using Filter Design and Analysis Tools from Simulink.

6.3 Combined observer

The combination of the modified voltage model and the high frequency signal injection approach is illustrated in the figure below.

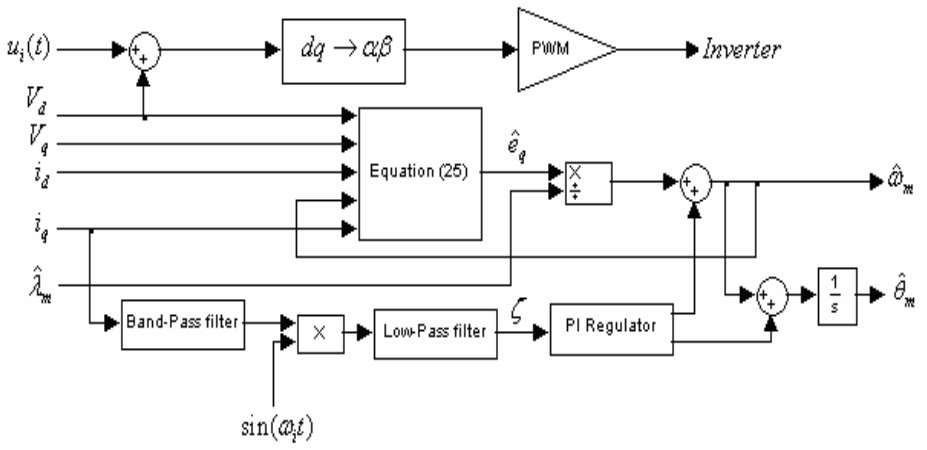

Figure 6.2:
Combined observer.

V_d, V_q, i_d and i_q can be obtained by transformation of the measured machine variables from the stationary reference frame to the rotor dq reference frame.
As mentioned in the previous paragraph, the error signal demodulated from the q-axis current component should be zero ($\zeta = 0$) during steady state, providing no error in the estimate rotor position. To meet this requirement, a PI-regulator is used to drive the error signal to zero during steady state. The integral gain of the regulator is used to adjust the estimated speed; meanwhile the proportional gain of the regulator is used to monitor the estimated rotor position. This arrangement is described by the following equation.

$$\hat{\omega}_m = \frac{\hat{e}_q}{\hat{\lambda}_m} + k_i \int \zeta \, dt$$
$$\hat{\theta}_m = \int (\hat{\omega}_m + k_p \zeta) dt \qquad (30)$$

Were k_i and k_p are positive gains.

6.4 Control system

The block diagram of the control system comprising the cascaded connection of the speed and current control loops is shown in the figure below. For position control, a P-type controller could be added as the outermost control loop in the control system.

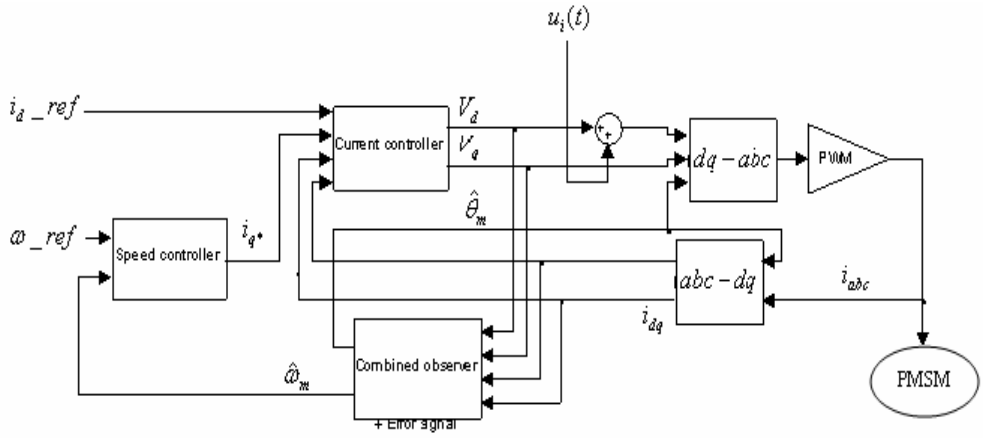

Figure 6.3: *Control system of the sensorless scheme with the proposed algorithm*

6.5 Simulation results

The proposed observer was investigated by mean of simulations, using Simulink (Matlab simulation tool). A 0.4 KW Surface Mounted Permanent Magnet Motor model was developed and used in Simulink. Inverter non linearity was not included in the model. The motor parameters are given in table 6.1. A reference speed approximately 8% of the rated speed was adopted, for convenient case of study at low speed range.

Table 6.1: *Motor parameters.*

Nominal power	0.4 KW
Nominal voltage	380 V
Nominal current	2 A
Nominal torque	1.3 Nm
Number of pole pairs	2
Stator resistance	$10.4\,\Omega$
Direct axis inductance	0.043 H
Quadrature axis inductance	0.043 H
Total moment of inertia	$0.94\ Kg.Cm^2$
Nominal speed	6000 rpm

Simulations results performed at different operating conditions of the machine are shown in the figure below.

Figure 6.4: *simulation results of the proposed algorithm at different operating conditions.*

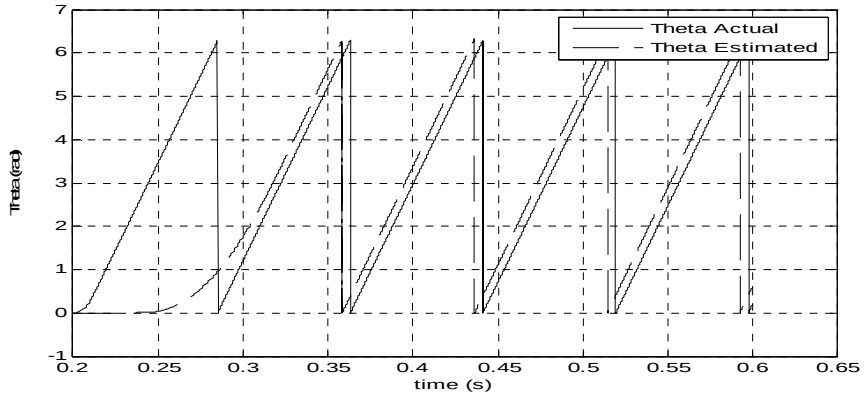

a) No load applied

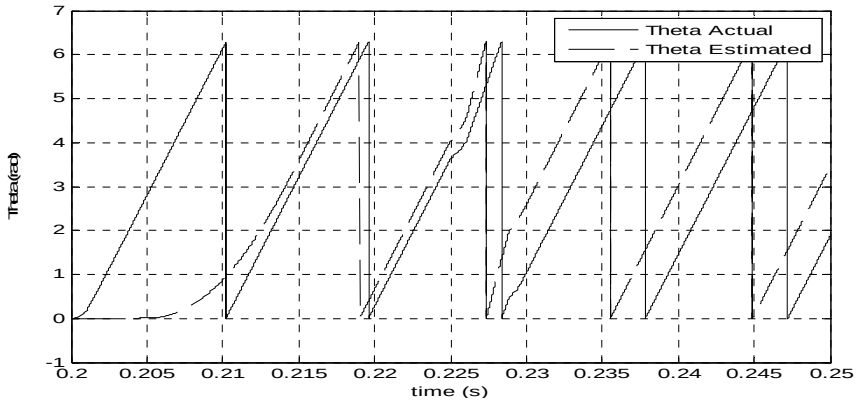

b) Step change in the reference speed, applied at 0.225 S.

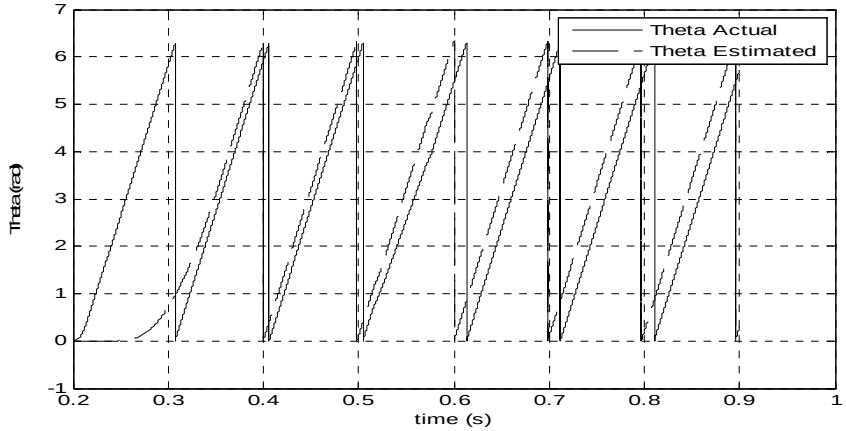

c) Step change in the load, applied at 0.53 S (approximately).

The result at no load (see fig 6.4 a), shows the effectiveness of the algorithm based on modified voltage model combined with high frequency signal injection. However it takes approximately 0.3 seconds for the observer to follow the rotor position. This delay could justify the limited robustness of the algorithm.

Figure 6.4 b shows the result with a step change in the reference speed, applied at 0.225 S. It can be seen from this figure that the change applied in the reference speed introduces large error in the rotor position estimation, thereby leading to a possibility to lose the rotor position in time.

In figure 6.4 c, a step change in the load was applied at 0.52 S (approximately). It results from this figure that the change in the load increases the error between the estimated rotor position and the actual rotor position. Thought the observer does not lose the rotor position, the increase in the error between the rotor positions could result in an unstable situation of the control system. This aspect could also prove the ineffectiveness of the algorithm in rejecting load torque transients.

Bibliography

[1] M. Corley and R. D. Lorenz, "Rotor position and velocity estimation for a salient-pole permanent magnet synchronous machine at standstill and high speeds," *IEEE Trans. Ind. Applicat.*, vol. 43, no. 4, pp. 784–78 July/Aug. 1998.

[2] L. Harnefors and H.-P. Nee, "A general algorithm for speed and position estimation of AC motors," *IEEE Trans. Ind. Electron.*, vol. 47, no. 1, pp. 77–83, Feb. 2000.

[3] M. Linke, R. Kennel, and J. Holtz, "Sensorless position control permanent magnet synchronous machines without limitation at zero speed," in *Proc. IEEE IECON'02*, vol. 1, Sevilla, Spain, Nov. 2002, pp. 674–679.

[4] J. H. Jang, S. K. Sul, J. I. Ha, K. Ide, and M. Sawamura, "Sensorless drive of SMPM motor by high frequency signal injection," in *Proc. IEEE APEC'02*, vol. 1, Dallas, TX, March 2002, pp. 279–285.

[5] F. Parasiliti, R. Petrella, and M. Tursini, "Sensorless speed control of salient rotor PM synchronous motor based on high frequency signal injection and kalman filter," in *Proc. IEEE ISIE'02*, vol. 2, L'Aquila, Italy, July 2002, pp. 623–628.

[6] H. Rasmussen, P. Vadstrup, and H. Borsting, "Sensorless field oriented control of a pm motor including zero speed," in *Proc. IEEE IEMDC'03*, vol. 2, Madison, WI, June. 2003, pp. 1224–1228.

[7] P. L. Jansen, M. J. Corley, and R. D. Lorenz, "Flux, position, and velocity estimation in ac machines at zero and low speed via tracking of high frequency saliencies," in *Proc. EPE'95*, vol. 3, Sevilla, Spain, Sept. 1995, pp. 154–159.

[8] L. Springob and J. Holtz, "High-bandwidth current control for torque ripple compensation in PM synchronous machines," *IEEE Trans. Ind. Electron.*, vol. 45, no. 5, pp. 713–721, Oct. 1998.

[9] R. B. Sepe and J. H. Lang, "Real-time observer-based (adaptive) control of a permanent-magnet synchronous motor without mechanical sensors, *IEEE Trans. Ind. Applicat.*, vol. 28, no. 6, pp. 1345–1352, Nov./Dec 1992.